

Thermal shape fluctuation effects in the description of hot nuclei

V. Martin

Análisis Numérico, Facultad de Informática, Universidad Politécnica de Madrid, 28660 Madrid, Spain

J.L. Egido and L.M. Robledo

Departamento de Física Teórica C-XI, Universidad Autónoma de Madrid, 28049 Madrid, Spain

(Dated: December 22, 2018)

The behavior of several nuclear properties with temperature is analyzed within the framework of the Finite Temperature Hartree-Fock-Bogoliubov (FTHFB) theory with the Gogny force and large configuration spaces. Thermal shape fluctuations in the quadrupole degree of freedom, around the mean field solution, are taken into account with the Landau prescription. As representative examples the nuclei ^{164}Er , ^{152}Dy and ^{192}Hg are studied. Numerical results for the superfluid to normal and deformed to spherical shape transitions are presented. We found a substantial effect of the fluctuations on the average value of several observables. In particular, we get a decrease in the critical temperature (T_c) for the shape transition as compared with the plain FTHFB prediction as well as a washing out of the shape transition signatures. The new values of T_c are closer to the ones found in Strutinsky calculations and with the Pairing Plus Quadrupole model Hamiltonian.

PACS numbers: 21.60.Jz, 21.10.Ky, 21.10.Ma

Introduction

Since the advent of the new generation of 4π gamma ray detectors and the improved accuracy in the channel selection new possibilities have opened up in the study of nuclear structure. Besides this, the availability of faster computers has made possible to perform realistic theoretical investigations with large configuration spaces. The high excitation energy is specially interesting since new features may take place. For example, in the quasicontinuum, the high level density gives rise to the unexpected phenomenon of the damping of the rotational motion. In the limit of high excitation energies (or temperature T) quantum effects become less relevant or may even disappear. Thus one expects that in a heated nucleus physical effects like superfluidity or shape deformations are washed out when T increases. This expectation can be easily understood in terms of the shell model since, by increasing T , one promotes particles from levels below the Fermi surface to levels above it. In the case of pairing correlations, blocking levels amounts to destroying Cooper pairs. In the case of shape deformation, by depopulating the deformation driving levels (intruders) one gets on the average less deformation. Experimental information about nuclear shape changes can be obtained by means of the Giant Dipole Resonance (GDR) built on excited states. Exclusive experiments studying the GDR strength at a given excitation energy (or T) of the nucleus have been carried out in refs. [1, 2, 3, 4]. The understanding of these phenomena is relevant because it affects important features like the fission barriers and the stability of the nucleus itself. For a recent review on hot nuclei see ref. [5].

The shape transitions have been object of many studies, most of them with *schematic models*, separable forces, and *small configuration spaces* [6, 7, 8, 9, 10]. The theoretical approaches used in the calculations are

based on the mean field approximation, mainly the Finite Temperature Hartree-Fock-Bogoliubov theory (FTHFB). The mean field approximations predict sharp shape transitions, whereas for finite systems, however, one expects washed out transitions instead. The fact that the predicted critical temperatures are rather high (around 2-3 MeV) indicates that not only the most probable deformation is relevant but that there is a finite (in some cases very large) probability for the system to have other shapes which should be taken into account. Calculations beyond mean field including thermal fluctuations have confirmed the expectation of washed out transitions [11, 12].

Theoretical studies with *effective forces* and *large configuration spaces* have been performed at the FTHFB level with density dependent forces, Skyrme [13, 14, 15] and recently with the Gogny [16] force. Additional calculations have been done in the relativistic mean field (RMF) approximation [17, 18]. Calculations including thermal fluctuations in conjunction with large configurations spaces and effective forces have been performed only very recently [17, 19].

From these studies a discrepancy has emerged since, while the *mean field approaches* (FTHFB) with *effective forces* (like Skyrme, the Gogny force or the relativistic approaches), provide the view of a sharp shape transition at a relatively high critical temperature ($T_c \approx 2.7$ MeV for ^{164}Er), schematic models (like the Pairing plus Quadrupole) and Strutinsky calculations provide also a sharp transition though at a much lower critical temperature ($T_c \approx 1.7$ MeV for ^{164}Er). Furthermore, the discordant point of a "sharp" transition for a small system, like the nucleus, predicted by both approaches requires further investigation. Earlier calculations with the Pairing plus Quadrupole Hamiltonian [11, 20] have pointed out the relevance of including fluctuations in mean field approaches at finite temperature as a step forward to clarify

some aspects of these problems. It is the aim of this paper to investigate the problems just mentioned as well as other related high excitation energy topics, level densities, etc., within a beyond mean field theory. Towards this end, the FTHFB calculations of ref. [16] with the Gogny force and large configuration spaces will be generalized to include fluctuations in the quadrupole moment degree of freedom.

The finite range density dependent Gogny force has the advantage of providing the particle-hole (Hartree-Fock) and the particle-particle (pairing) matrix elements from the same interaction, at variance with relativistic theories and most Skyrme calculations. In the fitting of the D1S [21] parametrization no excited states or spin dependent data was used, however, it has produced good results in the description of nuclear properties not only at zero [22, 23] but also at large spin [24] and, more recently [16], in calculations at high excitation energy. Since our purpose is to study the behavior of shell effects and fluctuations with temperature, we have selected both theoretically and experimentally well known nuclei that display a variety of shapes in the ground state: strongly deformed (¹⁶⁴Er), oblate (¹⁹²Hg) and rather soft (¹⁵²Dy).

Theory

To study the behavior of nuclei with increasing temperature we use the D1S [21] parametrization of the finite range density dependent Gogny force [22, 23] in the FTHFB framework [7, 25]. The Gogny force, at variance with most of the Skyrme parametrizations and the relativistic models, allows full selfconsistent calculations since it provides the particle-hole and pairing fields from the same force.

At finite temperature, as at temperature zero, the basic approximation is the mean field theory. Its most sophisticated version, the FTHFB, has been developed in refs. [7, 8, 26]. For convenience we will give here a short outline.

For a system at constant temperature T and with chemical potential μ , the equilibrium state can be obtained from the variational principle over the grand canonical potential

$$\Omega = E - TS - \mu N. \quad (1)$$

The energy, E , entropy, S , and particle number, N , are thermal averages defined by

$$\begin{aligned} E &\equiv \left\langle \hat{H} \right\rangle_T = \text{Tr}(\hat{D}\hat{H}), \\ S &\equiv \left\langle -k \ln \hat{D} \right\rangle_T = -k \text{Tr}(\hat{D} \ln \hat{D}), \\ N &\equiv \left\langle \hat{N} \right\rangle_T = \text{Tr}(\hat{D}\hat{N}), \end{aligned} \quad (2)$$

with Z the grand partition function and \hat{D} the density

operator given by

$$\begin{aligned} Z &= \text{Tr}[\exp(-\beta(\hat{H} - \mu\hat{N}))], \\ \hat{D} &= Z^{-1} \exp(-\beta(\hat{H} - \mu\hat{N})), \end{aligned} \quad (3)$$

with $\beta = 1/kT$.

In the FTHFB approach the density operator is approximated by

$$\hat{D}_0 = \frac{e^{\hat{\mathcal{H}}/T}}{Z_0}, \quad (4)$$

where $\hat{\mathcal{H}}$ is the most general Hermitian single particle operator, to be determined by the variational principle and Z_0 is the partition function. It can be shown [5] that \mathcal{H} is given by

$$\mathcal{H} = \begin{pmatrix} h & \Delta \\ -\Delta^* & -h^* \end{pmatrix}, \quad (5)$$

with Δ the pair potential and h the HF hamiltonian. h is given in terms of the kinetic energy t , the HF field, Γ , and the chemical potential, μ ,

$$\begin{aligned} h &= t + \Gamma - \mu, \\ \Gamma_{ij} &= \sum_{kl} v_{ikjl} \rho_{lk}, \\ \Delta_{ij} &= \frac{1}{2} \sum_{kl} v_{ijkl} \kappa_{kl}. \end{aligned} \quad (6)$$

The density matrix, ρ , and the pairing tensor, κ , are given by

$$\begin{aligned} \rho &= UfU^+ + V^*(1-f)V^t, \\ \kappa &= UfV^+ + V^*(1-f)U^t, \end{aligned} \quad (7)$$

and

$$f_i = \frac{1}{1 + e^{\beta E_i}}. \quad (8)$$

The matrices (U, V) provide the relation between the quasiparticle and the single particle basis :

$$\alpha_m^+ = \sum_k U_{km} c_k^+ + V_{km} c_k. \quad (9)$$

They are determined, together with the quasiparticle energies, E_i , by the FTHFB equation

$$\begin{pmatrix} h & \Delta \\ -\Delta^* & -h^* \end{pmatrix} \begin{pmatrix} U_k \\ V_k \end{pmatrix} = \begin{pmatrix} U_k \\ V_k \end{pmatrix} E_k. \quad (10)$$

The solution of this equations provides us with the configuration that minimizes the grand canonical potential. With U, V and f known one can determine the density operator \hat{D}_0 and calculate any expectation value. For density dependent forces like Skyrme or Gogny, the formalism remains unchanged except in the evaluation of the one body Hamiltonian h . Due to the dependence on the density of the interaction, h gets [19] an extra term, $\partial\Gamma$, which is usually referred to as the "rearrangement potential" and is given by

$$\partial\Gamma_{mm'} = \left\langle \frac{\partial H}{\partial \rho_{m'm}} \right\rangle_T. \quad (11)$$

The FTHFB solution gives us the most probable shapes, quadrupole, hexadecupole, etc, as well as the most probable gap parameters and so on. At finite temperatures, however, we have statistical (or thermal) fluctuations around this solution. In principle one could consider fluctuations in the most relevant degrees of freedom. For nuclei, at high excitation energy, the most important one is the quadrupole deformation, and we therefore shall consider only the fluctuations in the quadrupole moment $\langle \hat{Q}_{20} \rangle$ in this paper. To generate the solutions with different shapes we solve the grand canonical potential, Eq. (1), with an additional constraint on the quadrupole moment, i.e., we minimize $\Omega = E - TS - \mu N - \lambda_{Q_{20}} q$. The Lagrange multiplier $\lambda_{Q_{20}}$ is adjusted in such a way that the thermal expectation value $\langle \hat{Q}_{20} \rangle = \text{Tr}(\hat{D}\hat{Q}_{20})$, has the required value q . According to Landau [27] the probability $P(q)$ to obtain a certain value q of the deformation is characterized by the free energy $F(q) = E(q) - TS(q)$ of the system with deformation q

$$P(q) \propto e^{-F(q)/T}. \quad (12)$$

Using classical statistics, therefore, for the ensemble average of an observable $\hat{\mathcal{O}}$ one obtains the expression

$$\overline{\mathcal{O}} = \frac{\int \mathcal{O}(q) \exp(-F(q)/T) dq}{\int \exp(-F(q)/T) dq}, \quad (13)$$

where $\mathcal{O}(q)$ is the thermal expectation value of the operator $\hat{\mathcal{O}}$ calculated for the system with the deformation q , and dq is the volume element in deformation space. In our case the set q corresponds to the quadrupole deformation q_{20} , thus $dq = dq_{20}$, with metric equal to one. The limits in the thermal average integrals, see Eq. (13), are chosen to span the full β_2 region in which the probability of having one of these values, given by Eq. (12), is not negligible. This covers both prolate and oblate regions.

High temperature calculations require large configuration spaces. In order to maintain the computational burden within reasonable limits we restrict ourselves to axial symmetry. We are aware that for soft nuclei and/or high temperature, triaxiality may play an important role. In the calculations we use an axially deformed harmonic oscillator (HO) basis with a size defined by the condition

$$2b_\rho n_\rho + b_z n_z < N_0, \quad (14)$$

where n_ρ and n_z are the HO axial quantum numbers, $b_\rho = q^{1/3}$ and $b_z = q^{-2/3}$ with $q = R_z/R_\rho$, the nuclear axis ratio. In our case we have used $q = 1.5$ and $N_0 = 15$ which allows for deformations big enough to reach the fission barrier and provides room enough for the temperature induced excitations. However, as an additional check, we have also used $N_0 = 17$ for some selected calculations. Reflection asymmetry is allowed in the calculations, i.e. the nuclei may develop octupole deformations.

In order to compare our Gogny force results with the ones, more conventional and popular, of the schematic

Pairing plus Quadrupole model (PPQ), we have also performed calculations with this force. The configuration space (the spherical oscillator shells $N = 5, 6$ for neutrons and $N = 4, 5$ for protons) and the force parameters used are the one of Baranger-Kumar [28]. The calculations have been performed in exactly the same way as in ref. [12]

Results

We have performed FTHFB calculations with the D1S parameter set of the Gogny force in several nuclei to study the evolution of shell effects with temperature. Nuclei with different ground state deformations have been selected to illustrate their different behavior. As an example of a nucleus with a strongly prolate deformed ground state we used the thoroughly studied ^{164}Er . The soft $^{152}\text{Dy}_{86}$ is a transitional nucleus between the clearly spherical Dysprosium isotopes with $N \leq 84$ and the well deformed ones with $N \geq 88$. This nucleus was selected for its rich shell structure and shape coexistence. The heavier ^{192}Hg has been chosen due to its oblate ground state shape. The maximum temperature studied has been kept below 3 MeV, such that continuum contributions can be safely disregarded [29, 30].

The thermal fluctuations are represented through averages calculated according to Eq. (13). The deviations around the mean values can be studied by the standard deviation value

$$\sigma(\mathcal{O}) = \sqrt{\overline{\hat{\mathcal{O}}^2} - [\overline{\hat{\mathcal{O}}}]^2}. \quad (15)$$

This quantity is presented in some cases for further clarification of the results obtained.

Before entering in the discussion of the shape and pairing phase transitions we will start by presenting first a general view. In Fig. 1 we present the free energy, $F(\beta_2)$, and the quantity $P(\beta_2) \propto \exp(-F(\beta_2)/T)$ versus the quadrupole deformation, β_2 , at different temperatures. $P(\beta_2)$ provides the weight of a given shape β_2 in the evaluation of thermal average values. The results for ^{164}Er are displayed in the left column, for ^{152}Dy in the middle one and for ^{192}Hg in the right one. For the rare earth nuclei ^{164}Er and ^{152}Dy , where calculations within the two shells configuration space mentioned above are feasible, we also present results with the PPQ model. Results with the Gogny force are displayed by continuous lines and those with the PPQ force by dashed ones (thick lines represent $F(\beta_2)$ and thin ones $P(\beta_2)$). The well depths are measured from the point with $\beta_2 = 0$ and $P(\beta_2)$ has been normalized in such a way that the most probable deformation takes the value of unity.

Let us discuss first the low temperature calculations ($T = 0.3$ MeV) where we can observe the intrinsic shapes of the ground states. In the Gogny calculations for ^{164}Er there is a deep prolate minimum at $\beta_2 \approx 0.3$ and about 4.5 MeV higher an oblate one. With the PPQ model

the same gross features are observed, though the minima are not so deep. The probability distribution $P(\beta_2)$, however, is similar in both calculations. For the nucleus ^{152}Dy , in the Gogny case, the prolate minimum is at $\beta_2 \approx 0.15$ and a bit higher in energy the oblate one. The PPQ model, for this nucleus, provides a broad minimum around the spherical shape. $P(\beta_2)$, in contrast with ^{164}Er , looks quite different in the Gogny case than in the PPQ one. In both nuclei the free energy surfaces are broader with the Gogny force than with the PPQ one. For ^{192}Hg , we find the minimum at an oblate deformation of $\beta_2 \approx -0.15$ and about 1.7 MeV higher a small prolate minimum.

At higher temperatures the expected disappearance of shell effects becomes clear, in particular the vanishing of the barriers when several minima are available and the development of only one spherical minimum. Further finite temperature effects like the widening of the free energy curve and the more important role of fluctuations with increasing temperature appear in the Gogny calculations but not in the PPQ ones. In the PPQ case the free energy surfaces, with increasing temperatures, become flatter but not broader. They even become narrower! This unphysical effect has to do, obviously, with the size of the configuration space (two shells). As we can see already at ($T = 0.3$ MeV), at large deformations $F(\beta_2)$ increases very steeply because there are no orbitals with high- j (deformation driving) coming down. The mechanism to soften the free energy surface at high temperature by enhancing the probability to occupy high-lying orbitals (among them the high- j ones) works only with large configuration spaces. The anomalous behavior of $P(\beta_2)$ in ^{152}Dy , in the PPQ approach, at $T = 0.6$ MeV as compared with $T = 0.3$ MeV is due to the fact that at $T = 0.6$ the neutron pairing gap vanishes and the ground state becomes slightly prolate.

Figures 2, 5 and 6 show the detailed calculations for all three nuclei. These figures include both, the results at the FTHFB level and with shape fluctuations calculated as described above. Dashed lines and open symbols indicate the FTHFB results. Solid lines and filled symbols are used for averaged, fluctuations including, calculations. Figs. 5 and 6 show only Gogny results.

A. The nucleus ^{164}Er

In Fig. 2 we display the results of the calculations for the nucleus ^{164}Er with the Gogny force and with the PPQ model Hamiltonian. In panel (a) we show the self-consistent FTHFB (i.e., calculated with the solution of Eq. 10) and the averaged results (i.e., calculated according to Eq. 13) for the β_2 , β_4 and β_6 deformation parameters as a function of the temperature with the Gogny interaction. Let us first discuss the deformation parameter β_2 . For temperatures $0 < T < 1.0$ MeV, both predictions behave similarly, as one would expect for a nucleus with a well pronounced minimum. For tempera-

tures $1.0 < T < 2.0$ MeV, the FTHFB β_2 -values decrease rather smoothly while the averaged ones undergo a strong reduction. For $T > 2.0$ MeV the selfconsistent values decrease very steeply and collapse, finally, to zero deformation at $T = 2.7$ MeV. The averaged values, on the contrary, change tendency decreasing very smoothly in such a way that an almost constant value of β_2 is eventually obtained. The behavior of β_4 and β_6 is similar to the one of β_2 though not that spectacular. The same plot for β_2 but with the PPQ interaction is represented in panel (b). Quantitatively the main differences with the Gogny results are the faster collapse of the self-consistent value, at $T \approx 1.8$ MeV, and the reduction of the temperature interval where the averaged values are smaller than the selfconsistent ones. Looking at the probability distribution in Fig. 1 one can easily understand these differences. The temperature value at which the *mean field* (mf) deformation parameter collapses, which we will denote T_c^{mf} , has often been used in earlier mean field studies to signal a shape phase transition. It is obvious from panels (a) and (b) that in theories *beyond mean field* things look quite different and that definition of the critical temperature must be carefully considered. The big difference in T_c^{mf} as predicted by effective forces, like the Gogny force, and the PPQ is also known from calculations with Skyrme forces [13, 14] and the relativistic mean field approximation [17, 31].

The standard deviation in the deformation parameter β_2 , $\sigma(\beta_2)$, calculated according to Eq. 15, is presented in panel (c). One can distinguish three well defined zones : in the first one at low temperature, when pairing is still strong, the deformation is kept almost constant and fluctuations raise slowly. The Gogny and PPQ calculations predict about the same equilibrium shape in this zone. For temperatures higher than the one corresponding to the pairing collapse, $\sigma(\beta_2)$ increases rapidly up to a maximum value, remaining more or less at this value at higher temperatures. This step behavior is characteristic of a shape phase transition region. In fact, one could define the shape transition temperature as the one at which $\sigma(\beta_2)$ has a maximum. With this criterion one obtains $T = 1.4$ MeV for the PPQ result and $T = 1.7$ MeV in the Gogny case. Note the large difference in $\sigma(\beta_2)$ between the Gogny and PPQ results at high temperature. In this comparison, however, one must keep in mind that the PPQ model hamiltonian is restricted to a configuration space of two oscillator shells which strongly constraints the ability to produce fluctuations. This is clearly seen in Fig. 1 : the PPQ results rapidly develop a narrow parabolic shape with increasing temperature. This lack of fluctuations was already identified as partially responsible for the low multiplicity seen in the collective E2 quasi-continuum spectra in gamma decay calculations when compared to experiment [32, 33].

An additional confirmation of the importance of the fluctuations in calculations with the Gogny interaction as compared to the PPQ case is provided by the different behavior of the averaged deformation parameters with

respect to the mean field within the same model, see panels a) and b). The value of the average β_2 parameter at high temperatures illustrates the deviation of the free energy surface from a parabolic behavior. A value close to zero is expected for a parabola, e.g., in the PPQ case, while a larger one, as in the Gogny case, indicates the softness of the prolate side as compared with the oblate one. One should nevertheless keep in mind that only axially symmetric deformed shapes are allowed in the calculations.

In panel d) of Fig. 2, the proton and neutron pairing energies are displayed for the Gogny force. Up to $T \approx 0.2$ MeV the pairing energies are rather constant but for higher T values they decrease in absolute value very fast up to $T = 0.7$ MeV where they vanish. Thermal shape fluctuations, as expected in the low temperature regime, have little effect on the pairing correlations. Pairing fluctuations which would be more relevant [20] are not considered in this work.

It is interesting to take a look at the internal excitation energy, E^* , and also analyze it through the behavior of its derivative, the specific heat $C_V(T) = \partial E^*/\partial T$, since the appearance of peaks in this quantity is customarily interpreted as a signature in the search for phase transitions.

The evolution of E^* with temperature for both the FTHFB, E^* , and the average, \overline{E}^* , calculations, is presented in panels e) (Gogny force) and f) (PPQ force) of Fig. 2. With the Gogny force and in the low temperature regime, we can see the pairing collapse which is visible as a change in the slope of E^* . At higher temperatures a fairly quadratic behavior is observed in the excitation energy, which is slightly modified when the transition to the spherical phase takes place at high temperature around $T \sim 2.7$ MeV. There, a weaker change in the slope, hardly seen in the scale of the plot, is found. The change is more abrupt in E^* than in \overline{E}^* , again as expected in the picture of a thermally faded transition. The same facts are observed in the PPQ plot, where one can additionally observe that at high temperature the energy behaves more linear than quadratic as a function of T .

The different behavior of E^* and \overline{E}^* is also interesting : a) At temperatures below 0.8 MeV, both energy values coincide, b) between 0.8 MeV and the corresponding T_c^{mf} (around 2.7 MeV for Gogny and 1.8 MeV for PPQ), E^* is always below \overline{E}^* , c) at the critical temperature both energies do coincide and d) at higher temperatures they are rather similar. This behavior has a simple explanation if one considers the entropy as a function of the deformation at fixed temperature, see Fig. 3, and the fact that in general $F \leq \overline{F}$ [36], with F the selfconsistent FTHFB free energy at the given T . At low temperatures (≤ 0.8 MeV) and at temperatures above T_c^{mf} , the entropy is almost shape independent, i.e., $\overline{S} \approx S$ (with S the selfconsistent FTHFB entropy at the given T), and the free energy behaves like a parabola, $\overline{F} \approx F$, consequently $\overline{E}^* \approx E^*$. At temperatures $0.8 \leq T \leq T_c^{mf}$, $F < \overline{F}$ and $S < \overline{S}$, see Figs. 1 and 3, and consequently, since $\overline{F} = \overline{E} - T\overline{S}$,

$$E^* < \overline{E}^*.$$

The change in slope in \overline{E}^* as compared with E^* indicates that the corresponding specific heats, $\partial \overline{E}^*/\partial T$ and $\partial E^*/\partial T$, will be rather different. This can be seen in Fig. 4 where we observe two peaks in the selfconsistent results, both in the PPQ and in the Gogny calculations [37]. In between we find the typical linear behavior for a Fermi gas ($C_V = 2aT$). The low temperature peak is associated with the superfluid to normal transition and the high temperature one with the deformed to spherical shape transition. The low temperature peak remains nearly unaffected by the inclusion of fluctuations. At the mean field level this transition takes place at a temperature low enough such that shape fluctuations are irrelevant.

Comparing the FTHFB results with the PPQ force with those obtained with the Gogny interaction for the shape transition, we find again the different temperature predictions. Using as critical temperature, T_c , the temperature where C_V changes curvature, the same values are obtained as when the $\beta_2 = 0$ rule was used (1.8 MeV for PPQ vs. 2.7 MeV for Gogny). However, when fluctuations are taken into account, the difference in the predicted T_c by Gogny and PPQ gets smaller and the sharpness of the peaks reduced, indicating a less abrupt transition as is expected in a mesoscopic system. This is more evident in the Gogny results, where the peak becomes a broad bump, providing another clue of the greater importance of fluctuations in the Gogny case. By contrast, the PPQ peak, although broader than in the mean field case, is still sharp. Furthermore the PPQ specific heat levels off, showing how the limited configuration space available is a clear disadvantage of this model. If we now look for the changes in curvature we find $T_c = 1.4$ MeV in the PPQ and $T_c = 1.7$ MeV with the Gogny interaction. It is interesting to notice that these values agree very well with the ones obtained looking at $\sigma(\beta_2)$.

B. The nucleus ^{152}Dy

As we have seen in Fig. 1, ^{152}Dy displays a potential energy surface with energetically close prolate and oblate minima. It could illustrate a nucleus with shape coexistence, that means, already at temperatures near to zero there is a finite probability of populating more than one minimum. For this nucleus we will not perform a discussion as exhaustive as for ^{164}Er but we will consider the most relevant facts.

In Fig. 5 the results of the calculations for the Gogny force are displayed. In panel a) the mean field and the averaged values of the pairing energies are plotted. The pairing energy of the neutron (proton) system collapses at $T \approx 0.5$ ($T \approx 1.0$) MeV. The averaged values, as expected, almost coincide with the mean field ones. In panel b) the β -deformation parameters are shown. As we can observe in the behavior of the β_2 parameter the effect of the shape fluctuations in this case is already noticeable

at very small temperatures. This is due to the fact that, in the ground state ^{152}Dy is a much less deformed nucleus than ^{164}Er and that the energy difference between the oblate and prolate minimum is small, amounting to only ~ 0.55 MeV for $T < 0.5$ MeV. Hence the averaging formula assigns finite weights to the oblate side already at small T 's causing the observed steep decrease in the average β_2 value. Although the FTHFB, searching for the strict minimum, provides a deformed ground state for ^{152}Dy , we see how even at the lowest temperatures the average deformation is very small, in agreement with the experimental data. At the high temperature limit we observe that above 1.4 MeV, the average deformation stays rather constant, or slightly increases, up to 0.04. This anomalous behavior is due to the fact that the superdeformation driving orbitals are being occupied at this temperature range. The β_4 and β_6 deformation parameters follow closely the β_2 behavior. In particular, in the FTHFB description they become zero at the same temperature as β_2 .

In panel c) the excitation energy is depicted. In the FTHFB approach the changes in slope at temperatures of 0.5, 1.0 and 1.4 MeV are due to the neutron and proton pairing collapse and to the shape transition. The behavior of \bar{E}^* can be understood in terms of the entropy plots as explained for the ^{164}Er nucleus. The changes in slope in the energy plots are magnified in the specific heat versus temperature plot depicted in panel d). In the mean field approach we find a broad composite peak, corresponding to the proton and neutron pairing collapse, showing substructures around $T \approx 0.5$ and 1.0 MeV. Furthermore, one sees a second peak at 1.4 MeV corresponding to the FTHFB shape transition. If shape fluctuations are included in the calculations we obtain only one broad peak. The small peak at 1.4 MeV, however, is not there anymore indicating that it has been shifted to the pairing transition bump or simply washed out. In fact, the almost identical broad energy mean field peak and the single one obtained with fluctuations could be seen as a clue that the shape transition in this soft nucleus is nonexistent, since there is no higher temperature peak but only a small modification of the "pairing" one. To check this hypothesis we have also performed calculations with the particle-particle channel of the Gogny force set to zero, i.e. plain FTHF. In this way we obtain C_V curves without the pairing transition peaks. The results are plotted, superimposed to the standard FTHFB calculations, using square symbols in panel d) of Fig. 5. Again, open squares are for the FTHF calculations and full ones for averaged ones. As it was expected, the FTHF curves for C_V show no peak for the pairing transition and the only peak present is the one corresponding to the shape transition at 1.4 MeV, which coincides with the one obtained with the full FTHFB calculations, since at these temperatures pairing is already zero. The thermal averaging results show a broad shoulder approximately in the same temperature region in which the pairing transition was located. This rather soft bump is a clear indication

of the above mentioned situation, i.e., at small temperatures no clearly predominant minimum exists and at high temperatures the nucleus does not become exactly spherical.

C. The nucleus ^{192}Hg

As we have seen in Fig. 1 at very small temperatures this nucleus presents an oblate deformed ground state and about 1.7 MeV above a prolate minimum. The results for the nucleus ^{192}Hg are shown in Fig. 6. The pairing energies are displayed in panel a). The proximity of the $Z = 82$ shell closure causes the vanishing of the proton pairing energies for all temperatures. The neutron system, on the contrary, has a large pairing energy at $T = 0$ MeV, which vanishes at $T = 0.8$ MeV. As before, the shape fluctuations have almost no effect on the pairing energies.

In panel b) the behavior of the deformation parameters with increasing temperature is plotted. For ^{192}Hg , in the mean field approximation, we obtain an oblate ground state deformation of $\beta_2 = -0.135$ which gets more oblate for increasing temperatures as the pairing energies go to zero. For larger T values the deformation decreases and around $T \approx 1.4$ MeV the nucleus becomes spherical. As before, the effect of the shape fluctuations is mainly characterized by the the prolate-oblate ground state energy difference, see Fig. 1, which in this case amounts to 1.7 MeV at zero temperature and only above $T = 0.5$ MeV start to diminish. Around this temperature the deformation gets smaller and around 1.4 MeV the average deformation is zero. Interestingly, the average β_2 and β_4 deformation parameters become positive in the limit of high temperatures due to the fact that at these temperatures the $F(T)$ curves are softer in the prolate than in the oblate side.

In panel c) the excitation energies in both approximations, in the mean field and with shape fluctuations, are plotted versus the temperature. In the mean field calculations we find slope changes at $T = 0.8$ MeV and $T = 1.4$ MeV associated with the pairing collapse and the oblate-spherical shape transition. The inclusion of shape fluctuations affects mainly the region between $0.8 \leq T \leq 1.4$ MeV. The general behavior of both curves can be easily understood in the same terms as for ^{164}Er . In panel d) the corresponding specific heats are represented. In the mean field approximation the expected peaks are clearly visible. The inclusion of the shape fluctuations produces a single, broader bump extending above the critical temperature for the pairing collapse. As in the ^{152}Dy case this peak might be a superposition of the pairing and the shape transition peaks. To isolate the shape transition peak we have performed again calculations with the particle-particle channel of the Gogny force set to zero. The results of the calculations, without (empty squares) and with (filled squares) shape fluctuations, are represented in the same panel. In both approximations the

results above $T = 0.9$ MeV are obviously the same as before. Below this temperature and in the mean field approximation, as expected, the pairing peak is gone. However, in the calculations with the shape fluctuations we find a broad peak extending from $T = 0.4$ MeV up to $T = 1.0$ MeV with a change in curvature around $T = 0.9$ MeV. Looking at the standard deviation $\sigma(\beta_2)$ of this nucleus (not shown here) we find a maximum at $T = 0.9$ MeV, an additional indication of the shape transition.

D. Level densities and nuclear radii

Level densities, $\rho(E^*)$, can be microscopically evaluated in the saddle point approximation, see for example eq. (2B-14) of ref. [34]. In Fig. 7 the total level densities for the three nuclei under study are displayed against the excitation energy in the mean field approximation and on average, i.e., with the inclusion of shape fluctuations. In both cases we observe the overall expected exponential dependence and the well known abnormal behavior at very small excitation energies.

For ^{164}Er and up to 10 MeV excitation energy ($T \approx 0.8$ MeV) we find a good agreement between both predictions. Then, up to 70 MeV ($T \approx 2.3$ MeV), we observe an increase in the level density in the average description as compared with the mean field one. In particular, around 20 to 30 MeV excitation energy, the average prescription provides almost two orders of magnitude larger densities than the mean field one. This behavior can be easily understood looking at Figs. 1 and 3 and taking into account that the level density is proportional to the exponential of the entropy. At low ($T < 0.7$ MeV) and high excitation energies ($T > 2.5$ MeV) the entropy is rather shape independent, that means, the average value of the level density is very close to the one in the selfconsistent minimum. Consider now $T = 1.4$ MeV. In this case the selfconsistent minimum is prolate ($\beta_2 \approx 0.3$), and the entropy at this shape and T is smaller than for all the other shapes at this temperature. That means, since $\rho(\beta_2) \propto e^{S(\beta_2)}$, the average level density will always be larger than the selfconsistent one. Similar arguments apply to understand the behavior of the level densities of ^{152}Dy and ^{192}Hg . The fact that in these nuclei we do not find a larger difference between both descriptions is obviously due to the smoother behavior of the entropy with the deformation at the relevant temperatures.

In Fig. 8 the root mean squared (rms) radii of the three nuclei are plotted versus the temperature. In general we find that the rms radii are rather constant up to a given temperature, 2 MeV for ^{164}Er and 1 MeV for ^{152}Dy and ^{192}Hg , and that in this temperature range the average values are rather similar to the FTHFB ones. From this temperature on the average values are larger than the FTHFB ones due to the fact that, at these temperatures, the probability for a given shape peaks at the spherical shape and that for a given volume the spherical shape corresponds to the one with the smallest rms radii. That

means, fluctuations around the spherical minimum provide always larger rms radii. We also observe, at the highest temperatures, the expected increase of the rms radii.

Discussion and conclusions

We have seen in the previous section that, in calculating average properties, the behavior of the entropy with the deformation parameter β_2 plays a major role. This behavior is by itself, indeed, quite interesting. The general behavior, see Fig. 3, is the following : In the high T limit where the temperature effects dominate, we find, as expected, small shape dependence. At very low T , where the temperature effects are very small, we observe that to increase the entropy by 5 units we have to increase T by 0.5 MeV and that the entropy is rather independent of the shape of the nucleus. Of course, in this region where pairing correlations are present it is difficult to make more precise statements. However, at moderate temperatures, which are however high enough to allow for significant quasiparticle occupation numbers but not too high in order that shell effects are still present, one can find a large dependence of the entropy on the nuclear shape. In this region spherical shapes, as expected, have larger entropy than axially deformed ones. Since the maxima of the entropy are associated with the minima of the grand potential a correspondence between Fig. 1 and Fig. 3 does not necessarily exist.

One of the main outcomes of our research is the finding that shape fluctuations have a large effect on the description of shape transitions. In fact, the *mean field approach* (FTHFB) with effective forces (like Skyrme, the Gogny force or the relativistic approaches), provides the view of a sharp shape transition at a relatively high critical temperature ($T_c \approx 2.7$ MeV for ^{164}Er). On the other hand, Strutinsky calculations or schematic models (like the Pairing plus Quadrupole) provide also a sharp transition though at a much lower critical temperature ($T_c \approx 1.7$ MeV for ^{164}Er). It has been argued [18] that the different predictions for the critical temperature are due to the small effective mass obtained in the mean field approach with effective forces ($m^*/m \approx 0.7$, with m the nucleon bare mass) as compared to the Strutinsky or the PPQ model ($m^*/m \approx 1.0$). This argument is obviously restricted to the mean field approach. In theories beyond mean field it does not apply anymore because with increasing correlations the effective mass eventually becomes the bare mass. In calculations at finite temperatures two kinds of correlations have to be considered, on one hand the quantum ones and on the other the statistical or classical ones. Their relevance depends obviously on the excitation energy (or temperature), at low T 's the former are very important and at high T 's, the latter ones. At the temperatures where the shape transition is predicted to take place in the mean field approach, the probability of having a shape different to the selfconsis-

tent one is very large. Therefore, it is obvious that, first, shape fluctuations must be included and second that the characterization of the shape transition must be considered more carefully. In the mean field approach a criterion for shape transition is just to look at the temperature at which the nucleus becomes spherical or alternatively to look for a peak at the specific heat as a function of the temperature. In theories beyond mean field, usually the second one is used because the average deformation can become very small but not zero. As we have seen, the inclusion of shape fluctuations provides a specific heat rather different from the mean field one, because a) it is not a sharp peak what we obtain but a rather broad bump (this is consistent with the fact that it is a very small system) and b) it appears at temperatures much lower than the ones predicted by the mean field approximation in agreement with the Strutinsky calculations. It is also interesting to notice that the predictions based on the specific heat analysis coincide with the ones of the standard deviation $\sigma(\beta_2)$.

Of course one could ask about the effect of considering quantum correlations in our predictions. Canosa, Rossignoli and Ring [35] have shown in model calculations based on the static path plus random phase approximation that at finite temperature quantum effects are observable dependent. In particular, they find that the specific heat remains practically unaffected when quantum correlations are taken into account. One could conclude therefore that the prediction of the shape transition by the inclusion of thermal shape fluctuations with effective forces is

reliable.

In conclusion, we have performed extensive calculations with the Gogny force and a large configuration space for three representative nuclei in the FTHFB framework. We have further studied the effect of thermal shape fluctuations and found that they strongly affect, among others, the traditional shape transition "view" of the FTHFB approach. They do it in two aspects, first the critical temperature for the transition is very much lowered and second, the specific heat peaks are not sharp but rather broad. Besides this, the peaks showing up in FTHFB calculations of the specific heat in soft nuclei, like ^{152}Dy , are (almost) completely washed out when thermal shape fluctuations are taken into account indicating the absence of any shape transition. However, in strongly deformed nuclei, like ^{164}Er , the shape fluctuations re-confirmed the presence of a shape transition though of a different character. We also find a strong enhancement in the level density in the presence of a shape transition. The superfluid to normal phase transition is not affected by the inclusion of shape fluctuations.

Acknowledgments

This work has been supported in part by DGI, Ministerio de Ciencia y Tecnología, Spain, under Project BFM2001-0184.

[1] A. Atac, J. J. Gaardhje, B. Herskind, Y. Iwata, S. Ogaza, A. Bracco, A. M. Bruce, A. James, R. Chapman, F. Khazaie, et al., *Phys. Lett.* **252B**, 545 (1990).

[2] R. F. Noorman, J. C. Bacelar, M. N. Harakeh, W. H. A. Hesselink, H. J. Hofmann, N. Kalantar-Nayestanaki, J. P. S. van Schagen, A. Stolk, Z. Sujkowski, M. J. A. de Voigt, et al., *Phys. Lett.* **292B**, 257 (1992).

[3] V. Nanal, B. B. Back, D. J. Hofman, G. Hackman, D. Ackermann, S. Fischer, D. Henderson, R. V. F. Janssens, T. L. Khoo, A. A. Sonzogni, et al., *Nucl. Phys. A* **649**, 153c (1999).

[4] P. Heckman, D. Bazin, J. R. Beene, Y. Blumenfeld, M. J. Chromik, M. L. Halbert, J. F. Liang, E. Mohrmann, T. Nakamura, A. Navin, et al., *Phys. Lett.* **B555**, 43 (2003).

[5] J. L. Egido and P. Ring, *Jour. Phys. G* **19**, 1 (93).

[6] L. G. Moretto, *Phys. Lett.* **44B**, 494 (1973).

[7] A. L. Goodman, *Nucl. Phys. A* **352**, 30 (1981).

[8] J. L. Egido, P. Ring, and H. Mang, *Nucl. Phys. A* **451**, 77 (1986).

[9] A. L. Goodman, *Phys. Rev. C* **34**, 1942 (1986).

[10] R. Rossignoli and P. Ring, *Ann. Phys.* **235**, 350 (1994).

[11] J. Egido, C. Dorso, J. Rasmussen, and P. Ring, *Phys. Lett.* **178B**, 139 (1986).

[12] V. Martin and J. L. Egido, *Phys. Rev. C* **51**, 3084 (1995).

[13] M. Brack and P. Quentin, *Phys. Lett. B* **52**, 159 (1974).

[14] M. Brack and P. Quentin, *Phys. Scr.* **10**, 163 (1974).

[15] P. Quentin and H. Flocard, *Annu. Rev. Nucl. Part. Sci.* **28**, 523 (1978).

[16] J. L. Egido, L. M. Robledo, and V. Martin, *Phys. Rev. Lett.* **85**, 26 (2000).

[17] B. K. Agrawal, T. Sil, J. N. De, and S. K. Samaddar, *Phys. Rev. C* **62**, 44307 (2000).

[18] Y. Gambhir, J. Maharana, G. Lalazissis, C. Panos, and P. Ring, *Phys. Rev. C* **62**, 054610 (2000).

[19] V. Martin, J. Egido, and L. Robledo, in *Nuclear Physics, Nuclear Astrophysics. Proc. 3rd Int. Balkan School on Nuclear Physics*, edited by G. Lalazissis (Art of Text, Thessaloniki, 2003), p. 101.

[20] J. L. Egido, P. Ring, S. Iwasaki, and H. J. Mang, *Phys. Lett.* **154B**, 1 (1985).

[21] J. F. Berger, M. Girod, and D. Gogny, *Comput. Phys. Commun.* **63**, 365 (1991).

[22] D. Gogny, in *Nuclear Selfconsistent fields*, edited by G. Ripka and M. Porneuf (North-Holland, Amsterdam, 1975).

[23] J. Decharge and D. Gogny, *Phys. Rev C* **21**, 1568 (1980).

[24] L. M. Robledo and J. L. Egido, *Phys. Rev. Lett.* **85**, 1198 (2000).

[25] J. des Cloizeaux, in *Many Body Physics*, edited by D. de Witt and R. Balian (Gordon and Breach, New York, 1968).

[26] K. Tanabe, K. Sugawara-Tanabe, and H. J. Mang, Nucl. Phys. A **357**, 20, 45 (1981).

[27] L. Landau and E. Lifshitz, *Course of Theoretical Physics* (Pergamon Press, Oxford, 1959).

[28] K. Kumar and M. Baranger, Nucl. Phys. A **62**, 113 (1965).

[29] P. Bonche, S. Levit, and D. Vautherin, Nucl. Phys. A **427**, 278 (1984).

[30] P. Bonche, S. Levit, and D. Vautherin, Nucl. Phys. A **436**, 265 (1984).

[31] B. K. Agrawal, T. Sil, S. K. Samaddar, and J. N. De, Phys. Rev. C **63**, 24002 (2001).

[32] V. Martin, J. L. Egido, T. L. Khoo, and T. Lauritsen, Phys. Rev. C **51**, 3096 (1995).

[33] W. Ma, V. Martin, et al., Phys. Rev. Lett. **84**, 5967 (2000).

[34] A. Bohr and B. R. Mottelson, *Nuclear Structure* (Ben-jamin, Reading, Mass., 1975).

[35] N. Canosa, R. Rossignoli, and P. Ring, Phys. Rev. C **59**, 185 (1999).

[36] The equal sign is valid only in the case that the free energy is a parabolic function of the deformation.

[37] The results displayed in this figure have been calculated by evaluating numerically the derivative of the energy. In ref. [16] the expression $C_V = T\partial S/\partial T$ was used instead and S was calculated analytically in the mean field approach.

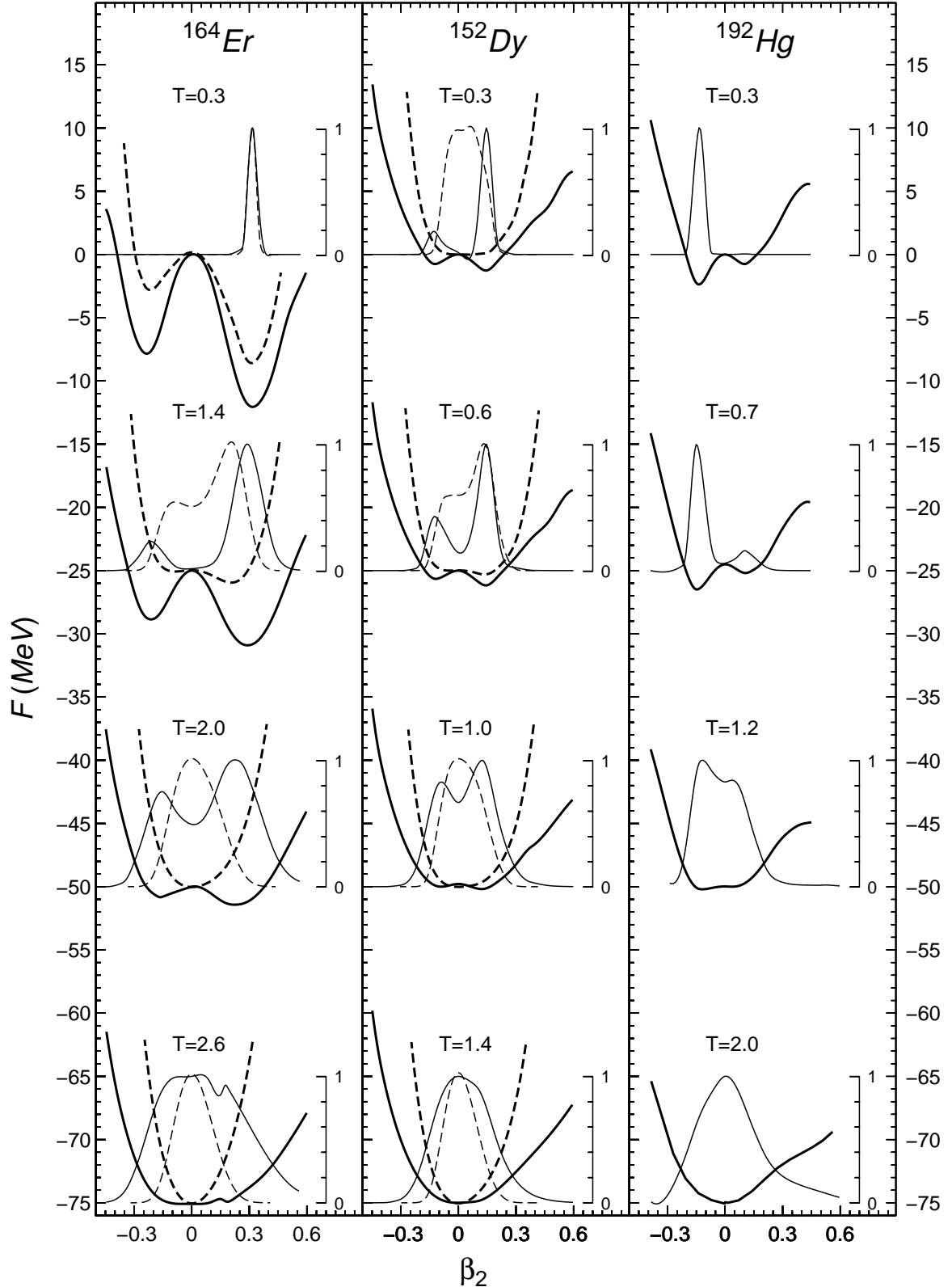


FIG. 1: Free energy curves for ^{164}Er , ^{152}Dy and ^{192}Hg calculated with the Gogny (thick solid lines) and PPQ (thick dashed lines) interactions at several temperatures as a function of the quadrupole deformation parameter β_2 . The probabilities $P(\beta_2)$ for a given shape β_2 , with the Gogny (thin solid lines) and the PPQ (thin dashed lines) interaction. The scale for $P(\beta_2)$ is given in the inset.

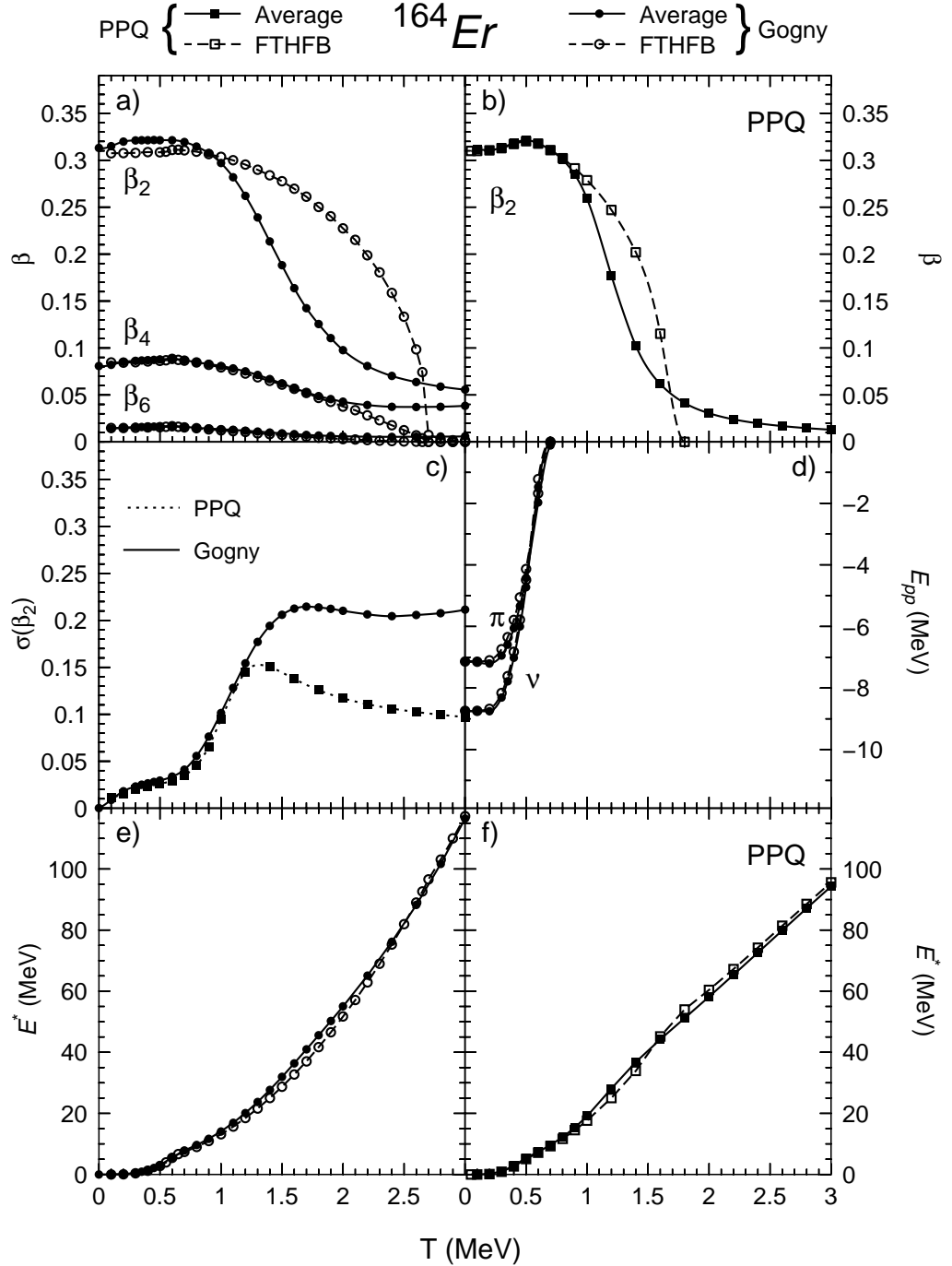


FIG. 2: Results for ^{164}Er for several observables as a function of the temperature. In all panels except in (d), solid lines and filled symbols are average values calculated according to Eq. 13, dashed lines and open symbols are for selfconsistent (FTHFB) results. Circles are for Gogny and squares for PPQ. Shown are the β_2 deformation parameter with Gogny (panel a) and PPQ (panel b) forces, the standard deviation $\sigma(\beta_2)$ with Gogny and PPQ forces (panel c), the pairing energies with the Gogny force (panel d) and the excitation energy with the Gogny (panel e) and the PPQ force (panel f).

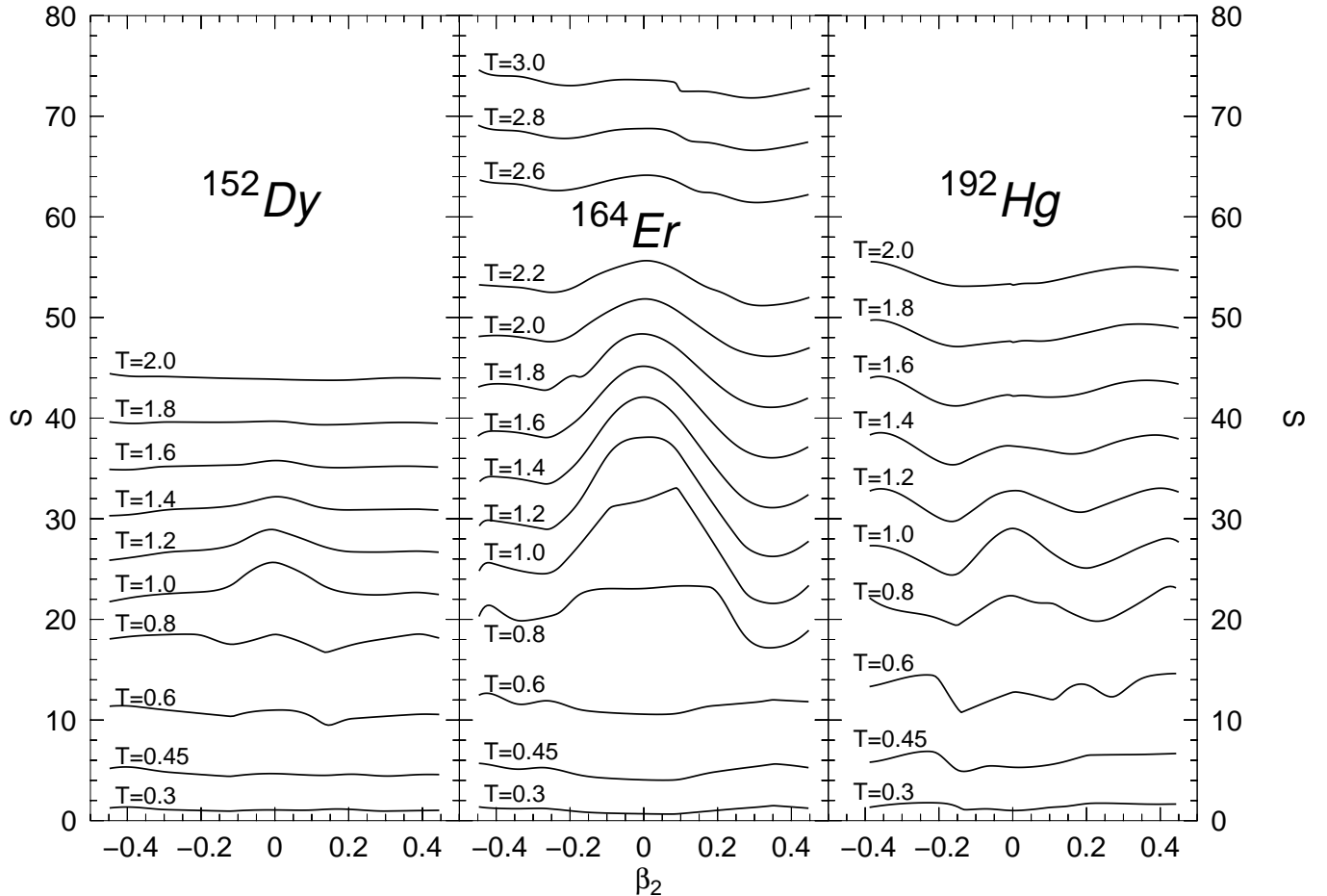


FIG. 3: The entropy at fixed temperatures as a function of the deformation parameter β_2 .

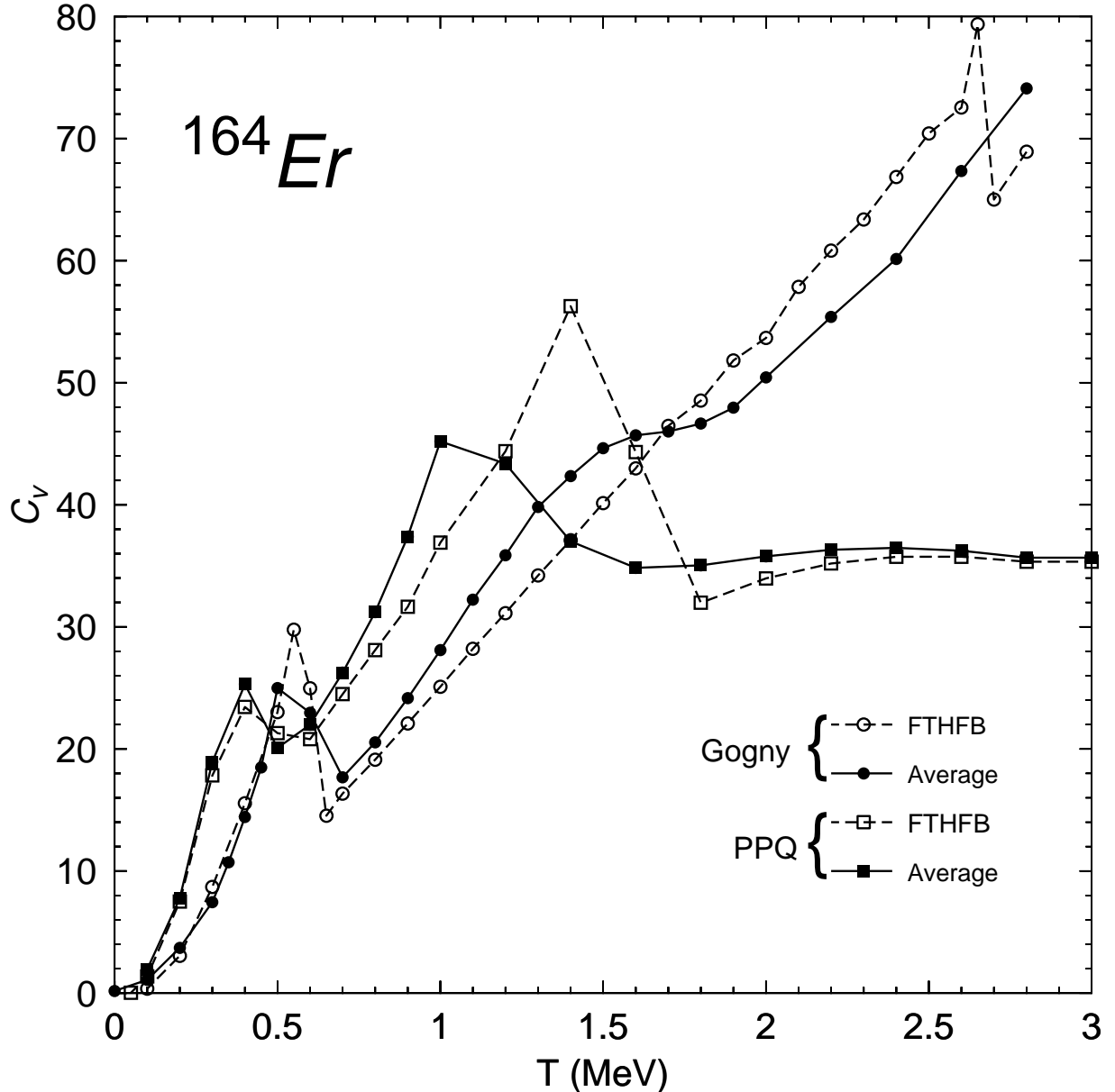


FIG. 4: The specific heat for the nucleus ^{164}Er with the Gogny (circles) and the PPQ (squares) interactions, in the FTHFB approximation (empty symbols) and the averages with shape fluctuations (filled symbols).

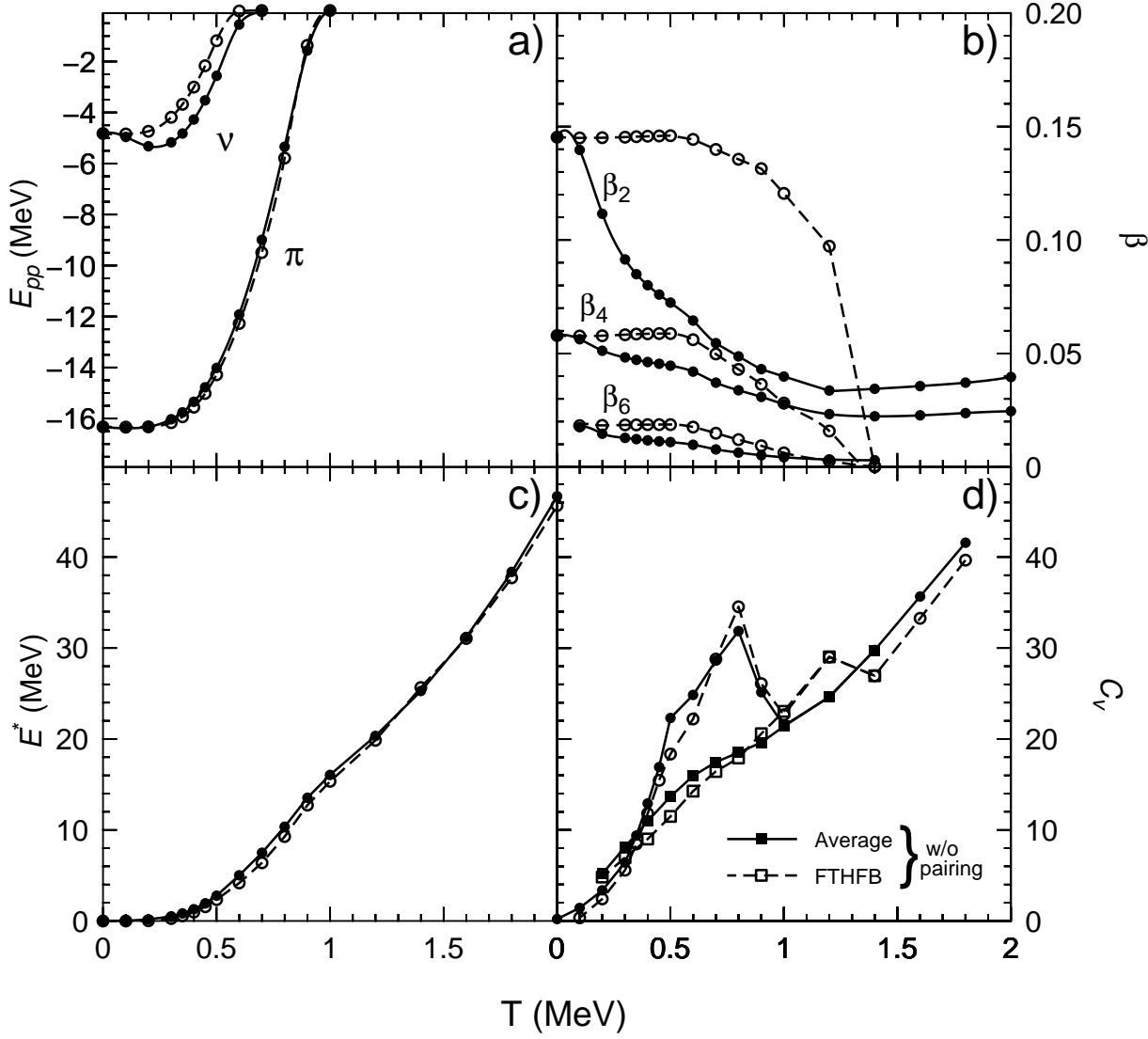


FIG. 5: Results for ^{152}Dy with the Gogny force versus the temperature. Average values are presented as solid lines and filled circles. Selfconsistent FTHFB results as dashed lines and open circles. Upper row, panel (a), pairing energies for protons π and neutrons ν . Panel (b), deformation parameters. Lower row, panel (c), excitation energies. Panel (d) specific heat calculated as defined in the text. Square symbols correspond to results using the Gogny force with pairing set to zero. In the temperature range from 1 to 1.5 MeV squares and circles are superimposed since above 1 MeV the solutions with and without pairing are the same.

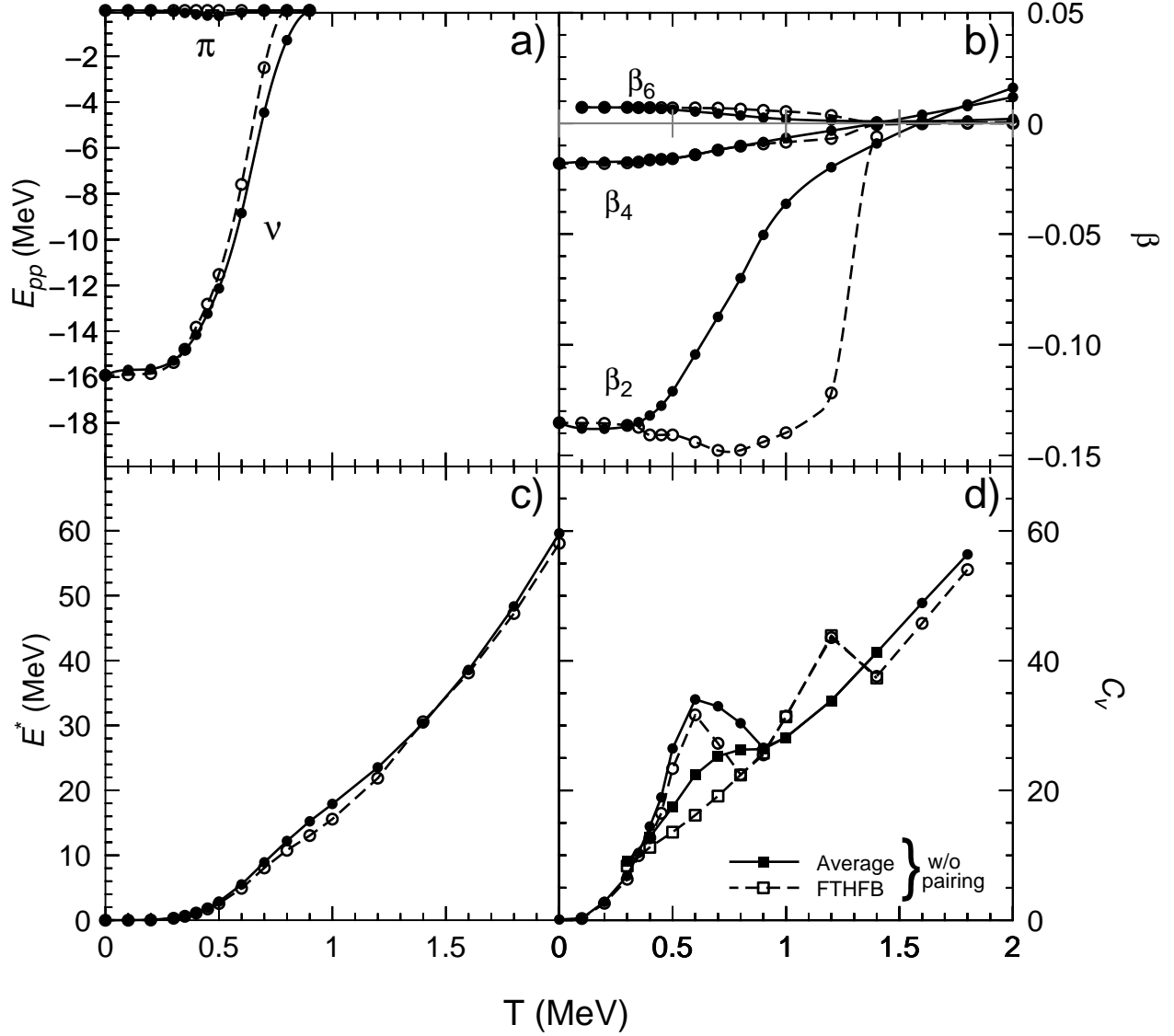


FIG. 6: Same than Fig. 5 for the nucleus ^{192}Hg . In panel (d) the superposition of results with and without pairing starts at $T=0.9$ MeV.

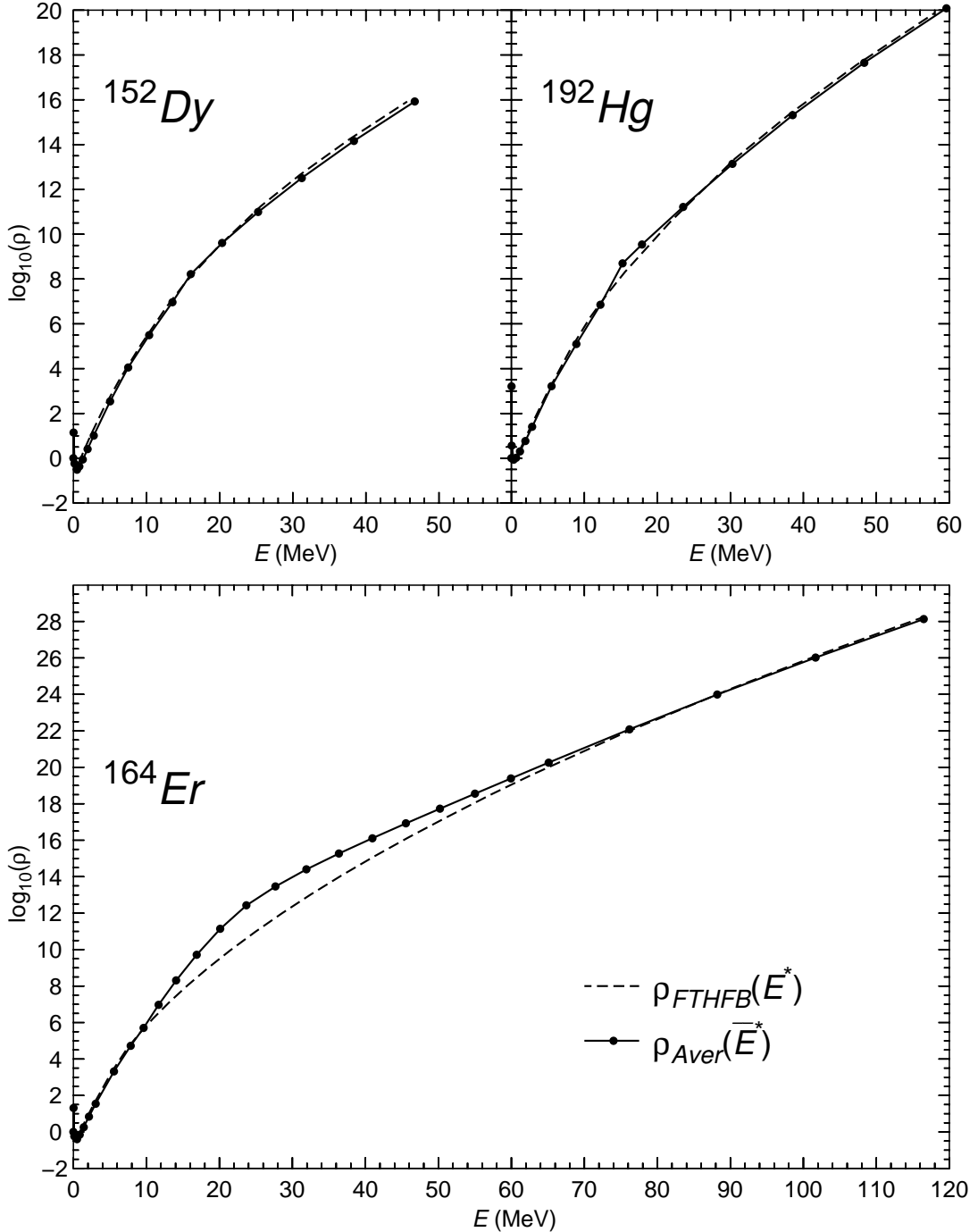


FIG. 7: Total level densities in MeV^{-1} versus the excitation energy for FTHFB (empty symbols) and averages with shape fluctuations (solid symbols).

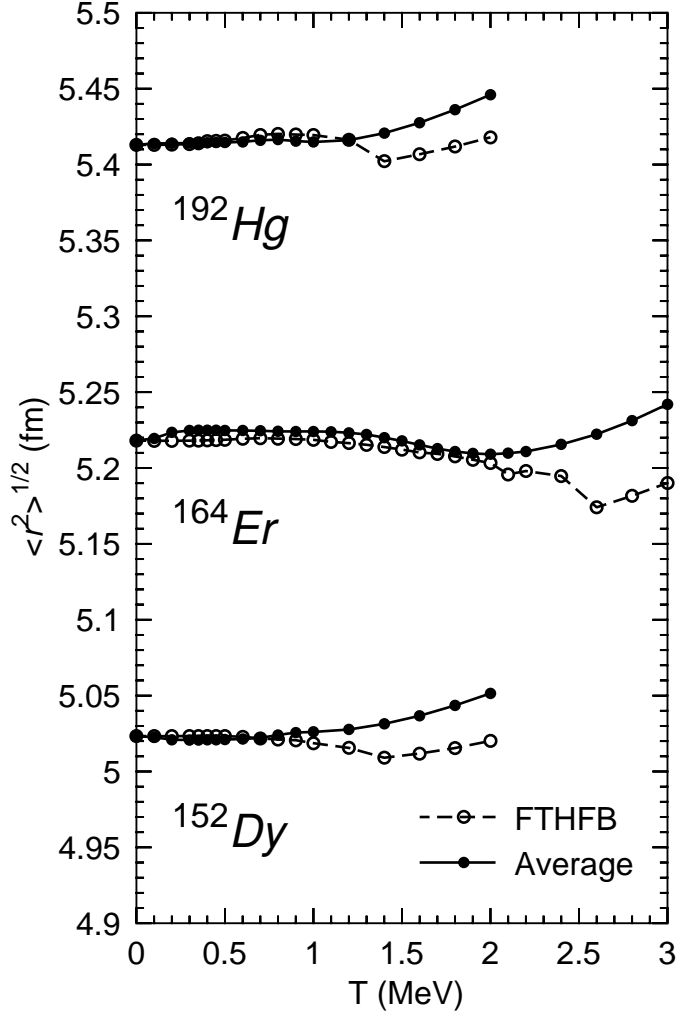


FIG. 8: Root mean squared radii, versus the temperature for FTHFB (empty symbols) and averages with shape fluctuations (solid symbols).